Mathematical Modeling of Emulsion Copolymerization Reactors

JOHN R. RICHARDS and JOHN P. CONGALIDIS, *Polymer Products Department, E. I. du Pont de Nemours and Company, Wilmington, Delaware, 19898,* and ROBERT G. GILBERT, *School of Chemistry, University of Sydney, NSW 2006, Australia*

Synopsis

This article presents the physical mechanism and the mathematical structure of a comprehensive dynamic emulsion polymerization model (EPM). EPM combines the theory of coagulative nucleation of homogeneously nucleated precursors with detailed species material and energy balances to calculate the time evolution of the concentration, size, and colloidal characteristics of latex particles; the monomer conversions; the copolymer composition; and molecular weight in an emulsion system. The capabilities of EPM are demonstrated by comparisons of its predictions with experimental data from the literature covering styrene and styrene/methyl methacrylate polymerizations. EPM can successfully simulate continuous and batch reactors over a wide range of initiator and added surfactant concentrations.

INTRODUCTION

The production of polymers by emulsion polymerization has been important since at least World War II. For example, the production of SBR, polybutadiene, and nitrile rubbers was 1.3 billion kg in 1983 in the United States alone.[1] Emulsion copolymers are important from an industrial viewpoint because they offer a unique mix of properties compared with homopolymers and can therefore open up new market opportunities. A review of the qualitative and quantitative aspects of emulsion polymerization can be found in reviews by Min and Ray[2] and more recently by Penlidis et al.[3] and Gilbert and Napper.[4]

Since the pioneering work of Smith and Ewart,[5] there has been a considerable effort to develop mathematical models for a fundamental understanding of emulsion homopolymerization. Significant contributions to this field have been added by the models of investigators such as Rawlings and Ray,[1] Min and Ray,[2] Hansen and Ugelstad,[6] Gilbert and Napper,[4] and Feeney et al.[7,8] For other work in the field the reader is directed to the review of Penlidis et al.[3]

Mathematical models for emulsion homopolymerization have been extended to copolymerization by investigators such as Haskell and Settlage,[9] Broadhead et al.,[10] Nomura and Fujita,[11] and more recently by Dougherty[12,13] and Storti et al.[14] Space does not permit a review of each of these articles.

Journal of Applied Polymer Science, Vol. 37, 2727–2756 (1989)
 CCC 0021-8995/89/092727-30$04.00

However, the main difference between their earlier work and the current article consists of (i) the development of a more comprehensive model in terms of particle formation mechanism and kinetic mechanisms with the extension of many of the existing literature equations from homopolymer to copolymer; (ii) applicability to intervals I, II, and III; (iii) the capability to simulate batch, semibatch, or continuous stirred tank reactors (CSTR); and (iv) isothermal and nonisothermal operation. Our aim has been to combine into a single coherent model the best aspects of previous models together with the coagulative nucleation theory of Feeney et al.[7,8] in order to enhance our understanding of this highly complex system.

MODEL STRUCTURE

The set of equations defining our emulsion polymerization model (EPM) will be presented in detail in the following sections (a preliminary version has been presented before[15] without the benefit of equations). Model results will then be compared to experimental data for styrene and styrene–methyl methacrylate (MMA) copolymers published by various investigators.

Physical Picture

The physical picture of emulsion copolymerization is complex due to the presence of multiple phases, multiple monomers, radical species, and other ingredients; complex particle formation mechanisms, and the possibility of many modes of reactor operation.

We begin the discussion of EPM by elaborating on this physical picture. Figure 1 shows a typical emulsion CSTR reactor and polymerization recipe. The magnified portion of the latex shows the various phases and the major species involved. The latex consists of monomers, water, surfactant, initiator, chain transfer agent, and added electrolyte. We use the mechanism for particle formation as described in Feeney et al.[7,8] These investigators took complete account of particle growth by coagulation of precursor particles formed by homogeneous nucleation. Their model is a significant extension of the "HUFT" nucleation theory of Hansen, Ugelstad, Fitch, and Tsai.[16] In our work, we have not found it necessary to invoke the micellar entry theory[1–3,5,10,12–14] to account for the number concentration of particles above the critical micelle concentration (CMC): Indeed, while micellar entry is frequently invoked, there is no unambiguous evidence for its kinetic significance, while there is a growing body of data that can only be interpreted in terms of a multistep nucleation model that incorporates coagulation of precursor particles.[7,8,17]

First, the water-soluble initiator decomposes to form free radicals in the aqueous phase. These free radicals then add to comonomers dissolved in the aqueous phase to start a free radical oligomer chain. If the monomers are present to a greater concentration than the saturation concentration and are only partially miscible with water, they will form a separate comonomer droplet phase. This phase then acts as a reservoir to feed the polymerization,

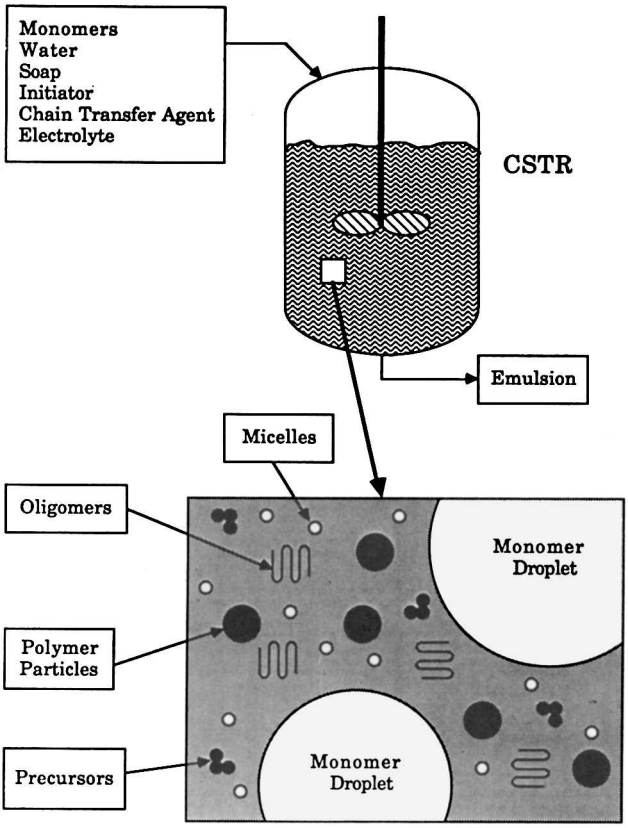

Fig. 1. The emulsion polymerization reactor.

which occurs in the polymer (latex) particles. Monomers distribute between the aqueous phase, the polymer particles, and the comonomer droplets.

The newly formed free radical oligomers propagate and may either enter polymer particles, enter precursors, terminate, or grow long enough so that they are no longer soluble in the aqueous phase. Then they drop out of solution and eventually become long enough to become primary precursors (homogeneous nucleation). These precursors are small (a few nanometers in size, and approximately spherical), colloidally unstable particles. These precursor particles have recently been directly observed[18] using small angle neutron scattering (SANS). The primary precursors coagulate and grow by polymerization to form k-fold precursors until they are large enough to be stable ($\approx$ 20 nm) and are then called latex particles. The latex particles are stabilized by initiator ionic end groups on the particle surface, by the adsorption of added surfactant (soap), and by the adsorption of terminated oligomers which act as *in situ* generated surfactant. The colloidally stable latex particles grow by polymerization to $\approx$ 100 nm. When the surfactant concentration is higher than the CMC, it forms a micelle phase, which in our analysis acts only as a soap reservoir.

When an aqueous phase radical enters the polymer particles, it becomes a polymer-phase radical, which reacts with a monomer molecule starting a propagating polymer chain. This chain may be stopped by chain transfer to monomer, by chain transfer to agent, or it may terminate by coupling. Small radicals in the particle may also desorb from or reenter the particle. In a batch reactor, interval I indicates the new particle formation period, interval II particle growth with no new particle formation, and in interval III the monomer droplets are absent.

The kinetic mechanism used for EPM is as follows. Note that it is assumed that the propagation and termination rates in the aqueous phase are the same as in the polymer phase.

Decomposition of initiator:

$$\mathrm{I} \xrightarrow{k_i} 2\mathrm{I}\cdot$$

Propagation in the aqueous phase:

$$\mathrm{A}_w\cdot + \mathrm{A}_w \xrightarrow{k_{paa}} \mathrm{A}_w\cdot$$
$$\mathrm{A}_w\cdot + \mathrm{B}_w \xrightarrow{k_{pab}} \mathrm{B}_w\cdot$$
$$\mathrm{B}_w\cdot + \mathrm{A}_w \xrightarrow{k_{pba}} \mathrm{A}_w\cdot$$
$$\mathrm{B}_w\cdot + \mathrm{B}_w \xrightarrow{k_{pbb}} \mathrm{B}_w\cdot$$

Termination in the aqueous phase:

$$\mathrm{A}_w\cdot + \mathrm{A}_w\cdot \xrightarrow{k_{taa}} \mathrm{Q}_w$$
$$\mathrm{A}_w\cdot + \mathrm{B}_w\cdot \xrightarrow{k_{tab}} \mathrm{Q}_w$$
$$\mathrm{B}_w\cdot + \mathrm{B}_w\cdot \xrightarrow{k_{tbb}} \mathrm{Q}_w$$

Homogeneous precursor formation:

$$\mathrm{A}_w\cdot^{j_{cr}-1} + \mathrm{A}_w \xrightarrow{k_{paa}} v_1$$
$$\mathrm{A}_w\cdot^{j_{cr}-1} + \mathrm{B}_w \xrightarrow{k_{pab}} v_1$$
$$\mathrm{B}_w\cdot^{j_{cr}-1} + \mathrm{A}_w \xrightarrow{k_{pba}} v_1$$
$$\mathrm{B}_w\cdot^{j_{cr}-1} + \mathrm{B}_w \xrightarrow{k_{pbb}} v_1$$

Coagulative nucleation: $k = 2, \ldots, m-1$

$$v_i + v_j \xrightarrow{B_{ij}} v_k$$

Entry of radicals into precursors:

$$\mathrm{A}_w\cdot + v_k \xrightarrow{k_{ea}} v_k$$
$$\mathrm{B}_w\cdot + v_k \xrightarrow{k_{eb}} v_k$$

Entry of radicals into particles:

$$\mathrm{A}_w\cdot + N_{i,j} \xrightarrow{k_{ea}} N_{i+1,j}$$
$$\mathrm{B}_w\cdot + N_{i,j} \xrightarrow{k_{eb}} N_{i,j+1}$$

Desorption of radicals:

$$N_{i,j} \xrightarrow{k_{da}} N_{i-1,j} + A_w \cdot$$
$$N_{i,j} \xrightarrow{k_{db}} N_{i,j-1} + B_w \cdot$$

Propagation in the polymer phase:

$$A_p \cdot + A_p \xrightarrow{k_{paa}} A_p \cdot$$
$$A_p \cdot + B_p \xrightarrow{k_{pab}} B_p \cdot$$
$$B_p \cdot + A_p \xrightarrow{k_{pba}} A_p \cdot$$
$$B_p \cdot + B_p \xrightarrow{k_{pbb}} B_p \cdot$$

Chain transfer to monomer in the polymer phase:

$$A_p \cdot + A_p \xrightarrow{k_{xaa}} A_p \cdot + Q_p$$
$$A_p \cdot + B_p \xrightarrow{k_{xab}} B_p \cdot + Q_p$$
$$B_p \cdot + A_p \xrightarrow{k_{xba}} A_p \cdot + Q_p$$
$$B_p \cdot + B_p \xrightarrow{k_{xbb}} B_p \cdot + Q_p$$

Chain transfer to agent in the polymer phase:

$$A_p \cdot + X_p \xrightarrow{k_{xax}} X_p \cdot + Q_p$$
$$B_p \cdot + X_p \xrightarrow{k_{xbx}} X_p \cdot + Q_p$$

Termination in the polymer phase

$$A_p \cdot + A_p \cdot \xrightarrow{k_{taa}} Q_p$$
$$A_p \cdot + B_p \cdot \xrightarrow{k_{tab}} Q_p$$
$$B_p \cdot + B_p \cdot \xrightarrow{k_{tbb}} Q_p$$

EPM has been developed to simulate as a function of time all the phases, species, and the detailed kinetic mechanism described in this section. The structure of EPM consists of material balances, the particle number concentration balance, phase volume balances, an energy balance, and the calculation of important secondary variables.

Material Balances

The following differential equations (1)–(10) give the time evolution of the molar concentration of each species in the reactor and assume that the reactor is perfectly mixed.[10] The species consist of water soluble initiator, added electrolyte, monomers A and B, chain transfer agent, added surfactant, *in situ* generated surfactant, monomers A and B in the dead (nonpropagating) polymer chains, and dead copolymer. In the case of a CSTR these equations consist of inflow, outflow, accumulation, and reaction terms. If there are no outflow terms, the equations reduce to semibatch operation. If in addition

there are no inflow terms, they reduce further to batch operation:

$$V_w\frac{dC_{iw}}{dt} = -C_{iw}\frac{dV_w}{dt} + F_i - C_{iw}Q_w - R_{iw}V_w \tag{1}$$

$$V_w\frac{dC_{yw}}{dt} = -C_{yw}\frac{dV_w}{dt} + F_y - C_{yw}Q_w \tag{2}$$

$$V_e\frac{dC_{ae}}{dt} = -C_{ae}\frac{dV_e}{dt} + F_a - C_{ae}Q_e - R_{pae}V_e \tag{3}$$

$$V_e\frac{dC_{be}}{dt} = -C_{be}\frac{dV_e}{dt} + F_b - C_{be}Q_e - R_{pbe}V_e \tag{4}$$

$$V_e\frac{dC_{xe}}{dt} = -C_{xe}\frac{dV_e}{dt} + F_x - C_{xe}Q_e - R_{pxe}V_e \tag{5}$$

$$V_e\frac{dC_{se}}{dt} = -C_{se}\frac{dV_e}{dt} + F_s - C_{se}Q_e \tag{6}$$

$$V_e\frac{dC_{ge}}{dt} = -C_{ge}\frac{dV_e}{dt} - C_{ge}Q_e + R_{ge}V_e \tag{7}$$

$$V_e\frac{dC_{aqe}}{dt} = -C_{aqe}\frac{dV_e}{dt} - C_{aqe}Q_e + R_{pae}V_e \tag{8}$$

$$V_e\frac{dC_{bqe}}{dt} = -C_{bqe}\frac{dV_e}{dt} - C_{bqe}Q_e + R_{pbe}V_e \tag{9}$$

$$V_e\frac{dC_{qe}}{dt} = -C_{qe}\frac{dV_e}{dt} - C_{qe}Q_e + R_{qe}V_e \tag{10}$$

Rate of Reactions

The rates of reaction that appear in the preceding material balances were calculated using the following equations (11)–(17) according to the mechanism given previously:

$$R_{iw} = k_iC_{iw} \tag{11}$$

$$R_{pae} = \left[(k_{paa} + k_{xaa})C_{a\cdot p}C_{ap} + (k_{pba} + k_{xba})C_{b\cdot p}C_{ap}\right]V_p/V_e \tag{12}$$

$$R_{pbe} = \left[(k_{pbb} + k_{xbb})C_{b\cdot p}C_{bp} + (k_{pab} + k_{xab})C_{a\cdot p}C_{bp}\right]V_p/V_e \tag{13}$$

$$R_{pxe} = \left[k_{xax}C_{a\cdot p}C_{xp} + k_{xbx}C_{b\cdot p}C_{xp}\right]V_p/V_e \tag{14}$$

$$R_{ge} = 2(1 - f)R_{iw}V_w/V_e \tag{15}$$

$$R_{ie} = 2fR_{iw}V_w/V_e \tag{16}$$

$$R_{qe} = R_{ie}/2 + R_{pxe} + \left[k_{xaa}C_{a\cdot p}C_{ap} + k_{xba}C_{b\cdot p}C_{ap} + k_{xbb}C_{b\cdot p}C_{bp} + k_{xab}C_{a\cdot p}C_{bp}\right]V_p/V_e \tag{17}$$

The kinetic rate constants were adjusted for temperature using the usual Arrhenius expression; for example,

$$k_{paa} = A_{paa}e^{(-E_{paa}/RT_e)} \tag{18}$$

These equations were derived using the appropriate kinetic constants, the concentrations of the reacting species in the polymer particles, and the concentrations of free radicals in the polymer particles. The rate of formation of *in situ* surfactant R_{ge} [eq. (15)] was assumed equal to the rate of formation of terminated oligomers in the aqueous phase. The derivation of the equation for the rate of formation of dead copolymer R_{qe} [equation (17)] presumes that each primary radical that enters a particle starts the growth of a new polymer chain, and that this chain is terminated almost immediately following capture of another radical.[19] The procedure for calculating the initiator efficiency f that appears in eqs. (15) and (16) will be discussed later.

Concentrations in Water and Particles

The equilibrium distribution of the two monomers and the chain transfer agent between the latex particles, the aqueous phase, and the comonomer droplets was described using empirical partition coefficients. An alternate, more complex, approach would be to use the rigorous thermodynamic treatment developed for copolymers by Krigbaum and Carpenter.[20] The volume of the separate monomer phase V_m is calculated from the total emulsion volume V_e and the volumes of the aqueous and polymer phases V_w and V_p as follows:

$$V_m = V_e - V_p - V_w \tag{19}$$

For species $j = a, b, x$, the partition coefficient K_{jwp} between aqueous phase and latex particles is defined[10] by the following equation:

$$K_{jwp} \equiv C_{jw}/C_{jp} \tag{20}$$

If there is a separate comonomer phase present ($V_m > 0$), partition coefficients K_{jmp} can also be defined between monomer droplets and polymer particles. If a single species j is present, the aqueous phase is saturated with j in interval II ($C_{jw} = C_{jw}^{\text{sat}}$). The following equation can therefore be derived to link the partition coefficients K_{jmp} and K_{jwp}:

$$K_{jmp} \equiv C_{jm}/C_{jp} = \rho_j K_{jwp}/M_j C_{jw}^{\text{sat}} \tag{21}$$

The concentration of species j in the polymer particles is calculated from the following equation:

$$C_{jp} = \frac{V_e C_{je}}{V_p + V_w K_{jwp} + V_m K_{jmp}} \tag{22}$$

The concentration of species j in the aqueous phase is given by

$$C_{jw} = K_{jwp}C_{jp} \tag{23}$$

Finally the volume fractions ϕ_j corresponding to the swelling of the polymer particle by species j can be calculated as follows:

$$\phi_j = C_{jp}M_j/\rho_j \tag{24}$$

Therefore, the volume fraction of the latex particle that consists of dead polymer ϕ_q is

$$\phi_q = 1 - \phi_a - \phi_b - \phi_x \tag{25}$$

Volumes of Aqueous and Particle Phases

The volumes of the aqueous and particle phases that appeared in eq. (19) together with the total volume of the emulsion were calculated by the following differential equations:

$$\frac{dV_e}{dt} = Q_f - Q_e + \Delta Q_e \tag{26}$$

$$C_{ww}\frac{dV_w}{dt} = F_w - \frac{Q_e V_w C_{ww}}{V_e} \tag{27}$$

$$\phi_q\rho_q\frac{dV_p}{dt} = -V_p\rho_q\frac{d\phi_q}{dt} - \frac{\phi_q\rho_q Q_e V_p}{V_e} + M_a R_{pae}V_e + M_b R_{pbe}V_e \tag{28}$$

The overall shrinkage ΔQ_e that appears in eq. (26) is caused by the different densities of the two monomers and the polymer and can be calculated as follows:

$$\Delta Q_e = \left(\frac{1}{\rho_q} - \frac{1}{\rho_a}\right)M_a R_{pae}V_e + \left(\frac{1}{\rho_q} - \frac{1}{\rho_b}\right)M_b R_{pbe}V_e \tag{29}$$

In the specific case of a liquid filled CSTR or one with perfect level control, the overall volume is constant ($dV_e/dt = 0$). Equation (26) can therefore be solved to express the volumetric reactor outflow Q_e in the terms of the reactor inflow Q_f and the shrinkage rate ΔQ_e:

$$Q_e = Q_f + \Delta Q_e \tag{30}$$

Since the molar concentrations of monomers and initiator in the aqueous phase are very small compared with the water concentration C_{ww}, the latter can be adequately approximated by the molar concentration of pure water as

follows:

$$C_{ww} \approx \rho_w / M_w \tag{31}$$

Radical Concentration in Particles

The radical concentration in the particles is also needed to calculate the reaction rates. EPM distinguishes between two types of free radical species in the particle, namely, radical chains ending with A · (concentration $C_{a \cdot p}$) and radical chains ending with B · (concentration $C_{b \cdot p}$). Using the quasi-steady-state hypothesis, the following equations were derived for $C_{a \cdot p}$ and $C_{b \cdot p}$ in terms of the average number of radicals (of any species) per particle, $\bar{n}$:

$$C_{a \cdot p} = \frac{\bar{n} N_e V_e}{V_p N_A} \left(\frac{1}{1 + \gamma_p} \right) \tag{32}$$

$$\gamma_p \equiv \frac{C_{b \cdot p}}{C_{a \cdot p}} = \frac{(k_{pab} + k_{xab}) C_{bp}}{(k_{pba} + k_{xba}) C_{ap}} \tag{33}$$

Following the procedure of Nomura and Fujita,[11] the steady state Smith–Ewart[5] equation for a copolymer system is as follows:

$$\begin{aligned} 0 = {} & \rho(N_{n-1} - N_n) + k_d[(n+1)N_{n+1} - nN_n] \\ & + c_t[(n+2)(n+1)N_{n+2} - n(n-1)N_n] \end{aligned} \tag{34}$$

As in the case of homopolymer, this equation accounts for entry of radicals into particles, radical desorption, and bimolecular termination. The kinetic constants ρ, k_d, and c_t that describe these events are related to the corresponding constants for homopolymerization by the following expressions:

$$\rho = \frac{R_{ie} N_A}{N_e} + \rho_{T_e} + \alpha k_d \bar{n} \tag{35}$$

$$k_d = (k_{da} + \gamma_p k_{db}) \left(\frac{1}{1 + \gamma_p} \right) \tag{36}$$

$$c_t = \frac{1}{2 v_p N_A} (k_{taa} + 2 k_{tab} \gamma_p + k_{tbb} \gamma_p^2) \left(\frac{1}{1 + \gamma_p} \right)^2 \tag{37}$$

The entry rate coefficient ρ in eq. (35) includes the entry of radical species formed by chemical initiation, background thermal initiation, and the reentry of desorbed radicals. The latter is described by the fate parameter[4] α which is related to the fate parameters of the pure monomers by the following equation which has been derived assuming a similar averaging procedure as

for desorption and termination:

$$\alpha = \frac{\alpha_a k_{da} + \alpha_b k_{db} \gamma_p}{k_{da} + k_{db} \gamma_p} \tag{38}$$

The fate parameter α takes complete account of whether desorbed free radicals undergo reentry and/or heteroterminate with radicals that would otherwise have entered the particles. A value of $\alpha = +1$ indicates that reentry is completely dominant. A value of $\alpha = -1$ indicates that heterotermination is completely dominant, and in general $-1 < \alpha < 1$. This fate parameter thus enables the encapsulation of complex aqueous phase kinetics in a single quantity. Extensive mathematical analysis[4] has shown that, to an excellent approximation, α is independent of $\bar{n}$.

The homopolymer termination constants that appear in eq. (37) were corrected for the Trommsdorff effect by using the following correlations proposed by Friis and Hamielec[21]:

$$k_{taa} = k_{taa0} \exp\left[2\left(k_{taa1}\chi_a + k_{taa2}\chi_a^2 + k_{taa3}\chi_a^3\right)\right] \tag{39}$$

$$k_{tbb} = k_{tbb0} \exp\left[2\left(k_{tbb1}\chi_b + k_{tbb2}\chi_b^2 + k_{tbb3}\chi_b^3\right)\right] \tag{40}$$

$$k_{tab} = \sqrt{k_{taa} k_{tbb}} \tag{41}$$

$$\chi_a = \frac{C_{aqe}}{C_{aqe} + C_{ae}} \tag{42}$$

$$\chi_b = \frac{C_{bqe}}{C_{bqe} + C_{be}} \tag{43}$$

These correlations express k_{taa} and k_{tbb} as a function of monomer conversions χ_a and χ_b and temperature T_e. The coefficient $1/(1 - \chi_b)$ in the original correlation has been deleted from eq. (40) (MMA) since is unreasonable to expect termination to become infinite at high conversion.[22] A rigorous theory for the prediction of the termination rate constant in free radical polymerizing systems at high conversions, which is based on the concept of center of mass diffusion and chain-end diffusion by propagational growth, is currently under development.[22] The cross-termination rate constant k_{tab} was approximated as the geometric mean of the two homopolymer termination constants.[19]

The homopolymer desorption coefficients in eq. (36) were calculated from the appropriate chain transfer constants and radical diffusivities in the aqueous and polymer phases using the desorption theory developed by Nomura and Fujita[11] and Hansen and Ugelstad.[23] The following equations were ap-

plied:

$$\frac{1}{k_{da}} = \frac{1}{\left[(k_{xaa} + k_{xba})C_{ap} + k_{xax}C_{xp}\right]} + \left[k_{0a}\left(\frac{k_{xaa}C_{ap} + k_{xba}k_{pab}C_{bp}/k_{pba} + k_{xax}C_{xp}}{k_{paa}C_{ap} + k_{0a}\bar{n} + k_{pab}C_{bp}}\right)\right]^{-1} \tag{44}$$

$$k_{0a} = \frac{3D_{wa}K_{awp}}{\left[r_p^2(1 + D_{wa}K_{awp}/2D_{pa})\right]} \tag{45}$$

$$\frac{1}{k_{db}} = \frac{1}{\left[(k_{xbb} + k_{xab})C_{bp} + k_{xbx}C_{xp}\right]} + \left[k_{0b}\left(\frac{k_{xbb}C_{bp} + k_{xab}k_{pba}C_{ap}/k_{pab} + k_{xbx}C_{xp}}{k_{pbb}C_{bp} + k_{0b}\bar{n} + k_{pba}C_{ap}}\right)\right]^{-1} \tag{46}$$

$$k_{0b} = \frac{3D_{wb}K_{bwp}}{\left[r_p^2\left(1 + \frac{D_{wb}K_{bwp}}{2D_{pb}}\right)\right]} \tag{47}$$

The first terms on the right-hand sides of eq. (44) and (46) have been derived in a manner similar to Hansen and Ugelstad[23] to cover the range where chemical reaction to produce small radicals is more important than the diffusional second term. The equations of Nomura and Fujita,[11] which are the second terms on the right-hand sides of eqs. (44) and (46), have been extended to include chain transfer to monomer and agent and represent the diffusion of the *small* radicals $X_p \cdot$ and $A_p \cdot$ out of the particles. Hence, chemical production of radicals by chain transfer to monomer and agent, diffusion inside the polymer particle to the surface competing with propagating a new polymer chain, and mass transfer through the aqueous exterior film of the particle constitute the mechanism used to derive the desorption equations.

The average number of radicals per particle, $\bar{n}$, can be calculated from eq. (34) using the following equation derived by O'Toole[24]:

$$\bar{n} \equiv \frac{\sum_{n=0}^{\infty} nN_n}{\sum_{n=0}^{\infty} N_n} = \frac{\xi I_\nu(\xi)}{4I_{\nu-1}(\xi)} \tag{48}$$

The order ν and the argument ξ of the modified Bessel function $I_\nu(\xi)$ of the preceding equation are defined by the following expressions:

$$\xi = (8\rho/c_t)^{1/2} \tag{49}$$

$$\nu = k_d/c_t \tag{50}$$

The numerical calculation of $\bar{n}$ was performed by using the following continued fraction expansion for $\bar{n}$ as suggested by Ugelstad et al.[25]:

$$\bar{n} = \frac{1}{2}\left\{\cfrac{\xi^2/4}{\nu + 0 + \cfrac{\xi^2/4}{\nu + 1 + \cfrac{\xi^2/4}{\nu + 2 + \cfrac{\xi^2/4}{\nu + 3 + \cfrac{\xi^2/4}{\nu + 4 + \cdots}}}}}\right\} \tag{51}$$

Particle Number Concentration Balance

In the development of EPM, we have assumed that the size dependence of the coagulation rate coefficients can be ignored above a certain maximum size, which should be chosen sufficiently large so as not to affect the final result. The following ordinary differential equation can be written to calculate the time evolution of the emulsion concentration of colloidally-stable latex particles of any size, N_e:

$$V_e\frac{dN_e}{dt} = -N_e\frac{dV_e}{dt} - N_eQ_e + G_{ce}V_e \tag{52}$$

The average particle volume v_p and the average radius of the monomer swollen and unswollen particle (r_p and r_q, respectively) can be calculated by the following expressions:

$$v_p = V_p/N_eV_e \tag{53}$$

$$r_p = \left(3v_p/4\pi\right)^{1/3} \tag{54}$$

$$r_q = r_p\phi_q^{1/3} \tag{55}$$

If the particle size distribution (PSD) of the latex particles is required, the population balance [eq. (52)] would have to be partial differential equation in volume and time, as shown by other investigators.[1,7,17] The PSD can also be computed by using the method of moments,[2] or directly from the calculated dN_e/dt as shown in the work of Feeney et al.[7]

The particle generation rate G_{ce} is calculated by a two-step mechanism, namely, formation of primary precursor particles by homogeneous nucleation[6] followed by coagulation and propagation to latex particles.[7,8]

Rate of Formation of Primary Precursors

The following steady state radical balance was used to calculate the concentration of the copolymer oligomer radicals in the aqueous phase $C_{a\cdot w}$ and $C_{b\cdot w}$:

$$2R_{iw} = R_{ew} + R_{tw} \tag{56}$$

This balance equates the radical generation rate $2R_{iw}$ with the sum of the rate of radical entry into the particles and precursors R_{ew}, and the rate of radical termination R_{tw}. Using the kinetic mechanism of the subsection, Material Balances, the following expressions can be written for these rates:

$$R_{ew} = k_{ea}\left(\frac{N_e}{N_A}\right)C_{a\cdot w} + k_{eb}\left(\frac{N_e}{N_A}\right)C_{b\cdot w} \tag{57}$$

$$R_{tw} = \tfrac{1}{2}k_{taa0}C_{a\cdot w}^2 + k_{tab0}C_{a\cdot w}C_{b\cdot w} + \tfrac{1}{2}k_{tbb0}C_{b\cdot w}^2 \tag{58}$$

$$k_{tab0} = \sqrt{k_{taa0}k_{tbb0}} \tag{59}$$

If these expressions are substituted back into eq. (56) together with eq. (11) for R_{iw}, the aqueous phase radical concentrations can be calculated by solving the resulting quadratic equation as follows:

$$C_{a\cdot w} = \frac{-\lambda_2 + \sqrt{\lambda_2^2 - 4\lambda_1\lambda_3}}{2\lambda_1} \tag{60}$$

$$\lambda_1 = \tfrac{1}{2}k_{taa0} + k_{tab0}\gamma_w + \tfrac{1}{2}k_{tbb0}\gamma_w^2 \tag{61}$$

$$\lambda_2 = (k_{ea} + k_{eb}\gamma_w)(N_e/N_A) \tag{62}$$

$$\lambda_3 = -2R_{iw} \tag{63}$$

$$\gamma_w \equiv \frac{C_{b\cdot w}}{C_{a\cdot w}} = \frac{k_{pab}C_{bw}}{k_{pba}C_{aw}} \tag{64}$$

The rate of propagation in the aqueous phase can be calculated by the following equation:

$$R_{pw} = k_{paa}C_{a\cdot w}C_{aw} + k_{pba}C_{b\cdot w}C_{aw} + k_{pab}C_{a\cdot w}C_{bw} + k_{pbb}C_{b\cdot w}C_{bw} \tag{65}$$

The entry rate coefficients k_{ea} and k_{eb} required for eq. (57) were calculated assuming that rate-controlling steps for radical entry are diffusion through a surface film and coagulative entry of oligomers, for which there is mounting experimental evidence, and thus that:

$$\frac{1}{k_{ea}} = \frac{1}{k_{ea}^{\max}} + \frac{1}{4\pi r_p^2 k_{ma}N_A + \beta_e B_{1m}N_A} \tag{66}$$

$$\frac{1}{k_{eb}} = \frac{1}{k_{eb}^{\max}} + \frac{1}{4\pi r_p^2 k_{mb}N_A + \beta_e B_{1m}N_A} \tag{67}$$

In eq. (66) $k_{ea}^{\max}$ is a maximum limiting value of the rate coefficient, k_{ma} is a surface mass-transfer coefficient, and $(\beta_e B_{1m}N_A)$ is a term representing bulk diffusion/electrostatic attraction/repulsion of an oligomer with a latex parti-

cle. Entry rate is hypothesized to be governed by mass transfer through a surface film ($4\pi r_p^2 k_{ma} N_A$) in parallel with bulk diffusion/electrostatic attraction/repulsion ($\beta_e B_{1m} N_A$) but in series with a limiting rate determining step ($k_{ea}^{\max}$). For styrene, this equation indicates that at high soap levels and large particles ($\gg$ 50 nm), the k_{ea} varies as ($4\pi r_p^2 k_{ma} N_A$). At low soap levels and small particles ($<$ 50 nm), the k_{ea} varies as ($\beta_e B_{1m} N_A$) or $k_{ea}^{\max}$, whichever is smaller. The parameter β_e takes on the value of 0 or 1 to switch on or off the coagulative entry contribution to the entry coefficient if desired. It is essential to note that the frequently adopted bulk diffusion theory[1] for the calculation of k_{ma}, which presupposes that *all* free radicals which collide with the particle are adsorbed, results in a value for k_{ea} which exceeds that experimentally observed[26] for large particles by many orders of magnitude.

The initiator efficiency f is defined as the ratio of the free radical entry rate to the total rate of radical generation:

$$f \equiv R_{ew}/R_{iw} \tag{68}$$

It should be pointed out that the aqueous phase radical balance in EPM provides a rigorous link between radical entry and initiator efficiency in contrast with previous models[1,10] that treated f and k_{ea} in eqs. (68) and (16) as independent adjustable parameters. There are other ways of defining f, but the present definition is one that is appropriate for an emulsion polymer system. It should be also noted that f is not directly measured in such systems, and in EPM f is purely an intermediate quantity in the calculations.

The radical entry rate, radical generation rate, and aqueous propagation rate were then used to develop the following algebraic equation for the rate of formation of primary precursors G_{he}:

$$G_{he} = \frac{2R_{iw}N_A(V_w/V_e)}{(1 + R_{ew}/R_{pw})^{j_{cr}-1}} \tag{69}$$

This equation is an extension to copolymers of the homogeneous nucleation equation derived by Hansen and Ugelstad[6] for a homopolymer.

According to the kinetic mechanism in EPM, primary precursor particles form when the degree of polymerization in the aqueous phase reaches a critical value j_{cr}. At this point the polymer chains become large enough to form an insoluble precursor particle of radius r_1. The following equations relate the size r_1 and volume v_1 of the primary precursor particles (of degree of polymerization j_{cr}):

$$j_{cr} = \frac{v_1 \rho_q N_A}{M_v} \tag{70}$$

$$v_1 = \tfrac{4}{3}\pi r_1^3 \tag{71}$$

$$M_v = \frac{M_a + (j_b/j_a)M_b}{(j_b/j_a) + 1} \tag{72}$$

$$\left(\frac{j_b}{j_a}\right) = \frac{(k_{pab} + k_{pbb}\gamma_w)C_{bw}}{(k_{paa} + k_{pba}\gamma_w)C_{aw}} \tag{73}$$

Particle Generation Rate

The primary precursor particles grow by propagation and coagulation until they reach a size that makes them colloidally stable. We denote by v_k the concentration of k-fold precursor particles, this is, precursor particles whose volume is k times the volume of the primary precursor particle v_1. When the number of primary precursor particles in a given precursor particle reaches a critical value m, this event corresponds to the formation of a colloidally stable latex particle. The latex particle generation rate G_{ce}, which is required to determine the concentration of latex particles N_e from eq. (52), can therefore be written as:

$$G_{ce} = \frac{1}{2}\sum_{i=1}^{m-1} v_i\left(\sum_{j=m-i}^{m-1} B_{ij}v_j\right) + \frac{K_{v\,m-1}v_{m-1}}{v_1} - 2B_{m,m}N_e^2 \tag{74}$$

This expression (which is similar to the equation derived by Feeney et al.[8]) contains terms corresponding to coagulation of precursor particles of volumes v_i and v_j, a term corresponding to volume growth of precursor particles by propagation and a term that represents the possibility of death of latex particles by flocculation. Care must be exercised to choose the value of the discretization parameter m sufficiently large so that the predicted value of the particle number is independent of m. The various factors that determine the colloidal stability characteristics of the latex particles (such as surfactant coverage[5]) are incorporated in the calculation of the coagulation coefficients B_{ij} as detailed in the succeeding sections.

The following equations were derived for a copolymer to calculate the volumetric growth rate by propagation of a k-fold precursor particle:

$$k = 1, \ldots, m-1$$

$$K_{vk} = \bar{n}_v\left[\frac{M_aC_{ap}(k_{paa} + k_{pba}\gamma_v) + M_bC_{bp}(k_{pab} + k_{pbb}\gamma_v)}{N_A\phi_q\rho_q(1+\gamma_v)}\right] \times \tanh\left(\frac{k^{1/3}r_1}{r_{FH}}\right) \tag{75}$$

$$\gamma_v \equiv \frac{C_{b\cdot v}}{C_{a\cdot v}} = \frac{k_{pab}C_{bp}}{k_{pba}C_{ap}} \tag{76}$$

The hyperbolic tangent term in eq. (75) takes into account the variation of monomer concentration inside the precursor particles with the radius of the particle; this variation is expressed in terms of a "Flory–Huggins radius" r_{FH}. The justification for introducing r_{FH} to calculate the monomer concentrations inside the precursor particles was provided by the work of Feeney et al.[8]

The procedures for calculating the concentrations of k-fold precursor particles v_k and the coagulation coefficients B_{ij} will be detailed in the following sections.

Number of k-Fold Precursor Particles

The following ordinary differential equations were written for the concentration of the k-fold precursors to account for birth and death by coagulation, growth by propagation, and the formation of primary precursors by homogeneous nucleation. There are $m - 1$ of these equations, which constitute a discretization of the partial integrodifferential equations for the particle size distribution of the precursors[8]:

$$k = 1, \ldots, m - 1$$

$$\frac{dv_k}{dt} = \frac{1}{2}\sum_{i=1}^{k-1} B_{i,k-1} v_i v_{k-i} - v_k \sum_{i=1}^{m-1} B_{i,k} v_i - B_{m,k} N_e v_k - \frac{K_{vk} v_k - K_{v\,k-1} v_{k-1}}{v_1} + \delta_{k,1} G_{he} \tag{77}$$

Coagulation Coefficients

The Müller coagulation coefficients are calculated by a lengthy procedure that is based on the theory of colloidal stability developed by Derjaguin, Landau, Verwey, and Overbeek (DLVO).[27] First, it is assumed the surface charge density σ_{vi} on the precursors and latex particles can be calculated by summing the contributions from the ionic end groups on the particle surface σ_{Ii}, and the absorbed surfactants σ_s (added) and σ_g (generated *in situ*). The following equation therefore holds:

$$\sigma_{vi} = \sigma_s + \sigma_g + \sigma_{Ii}, \qquad i = 1, \ldots, m \tag{78}$$

The ionic end group contribution σ_{Ii} was calculated by using the procedure described by Ottewill[28] by taking into account the fact that for the latex particles only a fraction ω of the end groups is on the particle surface and can therefore contribute to stabilization.[29] The following equations were derived:

$$r_i = i^{1/3} r_1, \qquad i = 1, \ldots, m - 1 \tag{79}$$

$$r_m = r_p \tag{80}$$

$$\sigma_{Ii} = \frac{\rho_q e_L N_A r_i}{3 M_v j_{cr}} \tag{81}$$

$$\sigma_{Im} = \frac{2 \rho_q e_L N_A r_p \omega}{3 M_q} \tag{82}$$

The number average molecular weight M_q needed for eq. (82) can be calculated from

$$M_q = \frac{C_{aqe} M_a + C_{bqe} M_b}{C_{qe}} \tag{83}$$

The surfactant contributions σ_s and σ_g were calculated by assuming that the adsorption of these species follows the multicomponent Langmuir isotherm for the surface coverage θ. The following equations were derived to compute the surface charge density in terms of the fraction of the particle surface covered by each surfactant:

$$\sigma_s = \frac{z_+ e_L \theta_s}{a_s'} \tag{84}$$

$$\sigma_g = \frac{z_+ e_L \theta_g}{a_g'} \tag{85}$$

$$\theta_g = \frac{b_g C_{gw}}{(1 + b_g C_{gw} + b_s C_{sw})} \tag{86}$$

$$\theta_s = \frac{b_s C_{sw}}{(1 + b_g C_{gw} + b_s C_{sw})} \tag{87}$$

The aqueous phase surfactant concentrations in eqs. (86) and (87) can be calculated from the following balances:

$$C_{gw} = \frac{C_{ge} V_e - (A_e \theta_g / a_g' N_A)}{V_w} \tag{88}$$

$$C_{sw} = \frac{C_{se} V_e - (A_e \theta_s / a_s' N_A)}{V_w} \tag{89}$$

The total surface area A_e of the particles and precursors is:

$$A_e = 4\pi r_p^2 N_e V_e + \sum_{k=1}^{m-1} 4\pi r_k^2 v_k V_e \tag{90}$$

Next, the surface potential was calculated using the Debye–Hückel[27] (low potential) formula for the precursors and the Gouy–Chapman[27] formula (high potential) for the particles. These equations are:

$$\Psi_{0i} = \frac{4\pi r_i \sigma_{vi}}{\epsilon(1 + \kappa r_i)}, \qquad i = 1, \ldots, m-1 \tag{91}$$

$$\Psi_{0m} = \left(\frac{2k_B T_e}{z_+ e_L}\right) \sinh^{-1}\left(\frac{2\pi e_L z_+ \sigma_{vm}}{\epsilon k_B T_e \kappa}\right) \tag{92}$$

The inverse thickness of the electric double layer κ in the preceding equations can be calculated from the ionic strength of the emulsion I_e and the permittivity ϵ of the dispersion medium using the following equations assum-

ing the symmetry of the initiator is 1 : 2 and the electrolyte is 1 : 1:

$$I_e \equiv \tfrac{1}{2}\sum_j \left(C_{+jw}z_{+jw}^2 + C_{-jw}z_{-jw}^2\right) = 3C_{iw} + C_{yw} \tag{93}$$

$$\epsilon = 4\pi\epsilon_0\epsilon_r \tag{94}$$

$$\kappa \equiv \left(8\pi e_L^2 N_A I_e/\epsilon k_B T_e\right)^{1/2} \tag{95}$$

By introducing the appropriate Stern layer thickness δ, the zeta potential[30] ζ_i can be calculated for the precursors and latex particles:

$$\zeta_i = \left(\frac{2k_BT_e}{z_+e_L}\right)\ln\left(\frac{e^{\lambda_4}+1}{e^{\lambda_4}-1}\right) \tag{96}$$

$$\lambda_4 = \kappa\delta + \ln\left(\frac{e^{\lambda_5}+1}{e^{\lambda_5}+1}\right) \tag{97}$$

$$\lambda_5 = \frac{z_+e_L\Psi_{0i}}{2k_BT_e} \tag{98}$$

It is therefore now possible to calculate the Hamaker[31] attractive potential energy Φ_A and the Hogg, Healy, and Fuerstenau[32] repulsive potential energy Φ_R for any latex particle/precursor pair in order to obtain the total energy Φ_T as a function of center to center separation distance R_{ij}:

$$i = 1, \ldots, m$$

$$j = 1, \ldots, i$$

$$R_{ij} = \frac{(r_i + r_j)s}{2} \tag{99}$$

$$L_{ij} = R_{ij} - (r_i + r_j) \tag{100}$$

$$\Phi_A = \frac{-A}{6}\left[\frac{2r_ir_j}{R_{ij}^2 - (r_i+r_j)^2} + \frac{2r_ir_j}{R_{ij}^2 - (r_i-r_j)^2} + \ln\left(\frac{R_{ij}^2 - (r_i+r_j)^2}{R_{ij}^2 - (r_i-r_j)^2}\right)\right] \tag{101}$$

$$\Phi_R = \frac{\epsilon r_ir_j\left(\zeta_i^2 + \zeta_j^2\right)}{4(r_i+r_j)}\left[\frac{2\zeta_i\zeta_j}{\left(\zeta_i^2+\zeta_j^2\right)}\ln\left(\frac{1+e^{-\kappa L_{ij}}}{1-e^{-\kappa L_{ij}}}\right) + \ln(1-e^{-2\kappa L_{ij}})\right] \tag{102}$$

The maximum of the potential energy curve $\Phi_{T\max}$ was found and the Fuchs stability ratio[28] W_{ij} was calculated as follows:

$$\Phi_{T\max} = \max_s(\Phi_T(s)) = \max_s(\Phi_A(s) + \Phi_R(s)) \tag{103}$$

$$W_{ij} = W_{ji} = 2\int_2^\infty \left\{ \frac{e^{(\Phi_T(s)/k_BT_e)}}{s^2} \right\} ds \tag{104}$$

$$W_{ij} \approx \left(\frac{r_i + r_j}{4\kappa r_i r_j} \right) e^{(\Phi_{T\max}/k_BT_e)} \tag{105}$$

Finally, the coagulation coefficient B_{ij} for each particle and precursor size pair was calculated using the Müller equation[33]:

$$B_{ij} = B_{ji} = \left(\frac{2r_j k_B T_e}{3r_i \mu W_{ij}} \right) \left(1 + \frac{r_i}{r_j} \right)^2 \tag{106}$$

Energy Balance

A dynamic differential equation energy balance was written taking into account enthalpy accumulation, inflow, outflow, heats of reaction, and removal through a cooling jacket. This balance can be used to calculate the reactor temperature in nonisothermal operation.

Case 1: nonisothermal:

$$V_e\rho_e c_e \frac{dT_e}{dt} = \rho_f c_f Q_f T_f - \rho_e c_e Q_e T_e + (-\Delta H_{pa}) R_{pae} V_e M_a + (-\Delta H_{pb}) R_{pbe} V_e M_b - U_j A_j (T_e - T_j) \tag{107}$$

Case 2: isothermal:

$$\frac{dT_e}{dt} \equiv 0 \tag{108}$$

Secondary Variables

Once the primary variables were obtained, numerous secondary variables were also calculated such as the polymer composition X_a and the overall copolymer conversion χ. The following equations were used in the calculations:

$$X_a = \frac{C_{aqe}M_a}{C_{aqe}M_a + C_{bqe}M_b} \tag{109}$$

$$\chi = \frac{C_{aqe}M_a + C_{bqe}M_b}{C_{aqe}M_a + C_{bqe}M_b + C_{ae}M_a + C_{be}M_b} \tag{110}$$

Numerical Implementation

The preceding eqs. (1)–(110) form a stiff set of nonlinear algebraic and ordinary differential equations which were integrated numerically using the Gear algorithm.[34] Since ρ is a function of $\bar{n}$ as shown in eq. (35), eqs. (35)–(51) were solved iteratively for $\bar{n}$ using a Wegstein procedure. Equations (86)–(89) were solved simultaneously for the four unknowns $\theta_g, \theta_s, C_{gw}, C_{sw}$ using a nonlinear equation solver.[34] The particle number concentration balance [eq. (52)] was scaled by a large number ($\approx N_e$) to facilitate the integration process. The Müller coagulation coefficients [eqs. (99)–(106)] were only updated at appropriate fixed time intervals on the order of a few seconds to speed up the computations. The maximum of the potential energy curve $\Phi_{T\max}$ [eqs. (99)–(103)] was found using a maximizer routine.[34] The derivative $d\phi_q/dt$ in eq. (28) was approximated by a filtered first-order finite difference as follows:

$$\left[\frac{d\phi_q}{dt}\right]_t = \tau\left[\frac{\Delta\phi_q}{\Delta t}\right]_t + (1-\tau)\left[\frac{\Delta\phi_q}{\Delta r}\right]_{t-\Delta t} \tag{111}$$

The filter factor τ in the preceding equation was chosen as $\tau = 0.3$ to eliminate high frequency noise generated in the derivative approximation. If $\tau = 1$, no filtering is done. More filtering is achieved as $\tau \to 0$ and in the limit only the initial value is retained.

The Cray X-MP™ supercomputer was used for the calculations reported in this paper with the computation time for a typical case about 5 min.

RESULTS

There is an enormous amount of data in the literature on the effect of many factors (temperature, monomer and surfactant concentration and types, ionic strength, reactor configuration, etc.) on the time evolution of quantities such as conversions, particle number and size, molecular weight, composition, and so on. In this section, EPM predictions are compared with the following limited but useful cross section of isothermal experimental data:

- Goodwin et al.[35] (Figs. 2 and 3) styrene homopolymerization in a batch reactor at 70°C with no added surfactant.

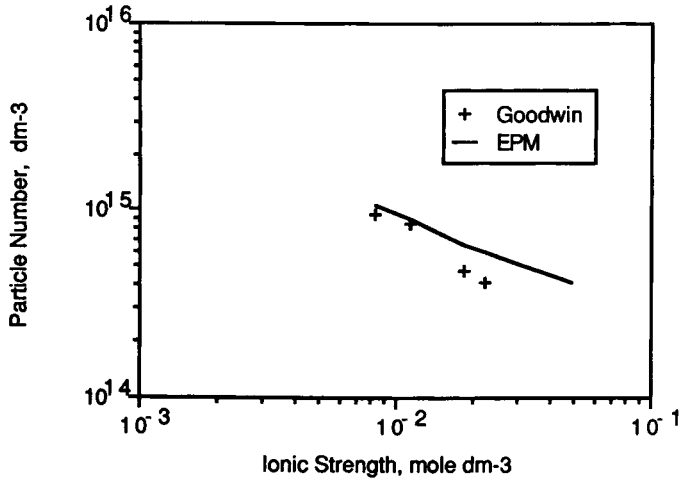

Fig. 2. Particle number vs. ionic strength for the data of Goodwin et al.[35] (+): (−) EPM.

- Sütterlin[36] (Figs. 4 and 5), styrene homopolymerization in a batch reactor at 80°C with various amounts of added surfactant.
- Badder and Brooks[37] (Fig. 6) styrene homopolymerization in a CSTR at 50°C with added surfactant.
- Nomura and Fujita[11] (Figs. 7 and 8) styrene/MMA copolymerization in a batch reactor at 50°C using speed particles.

Since both these monomers have been extensively studied, we simulated the experiments by using the same set of parameters for all runs except as noted in the discussions of the figures. Parameters for all of these runs were obtained from the literature. Values together with the corresponding literature references of all parameters are given in Table I.

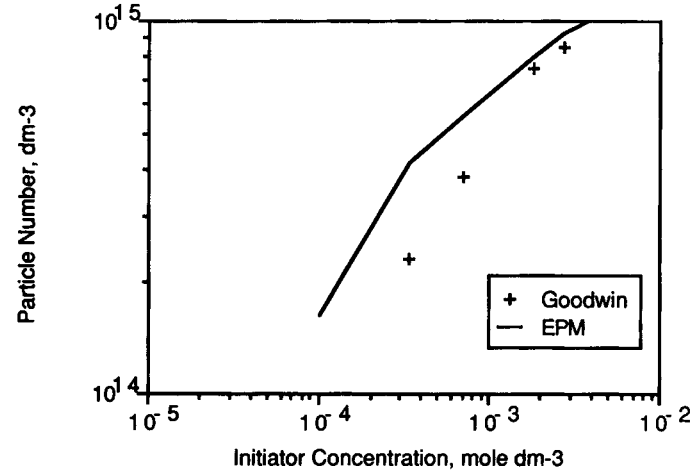

Fig. 3. Particle number vs. initiator concentration for the data of Goodwin et al.[35] (+): (−) EPM.

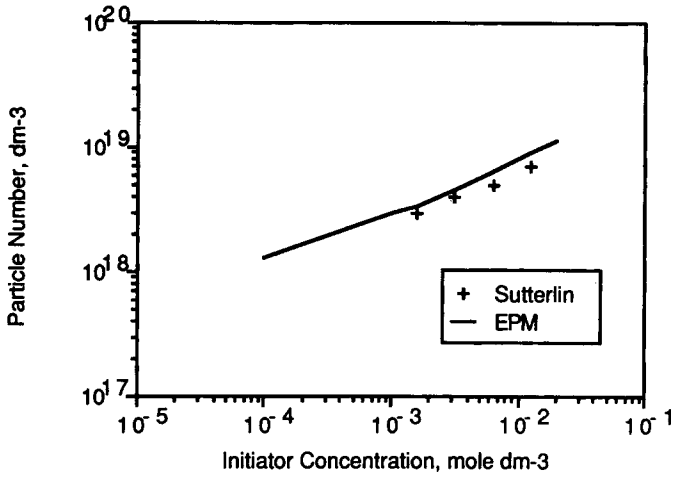

Fig. 4. Particle number vs. initiator concentration for the data of Sütterlin[36] (+): (−) EPM.

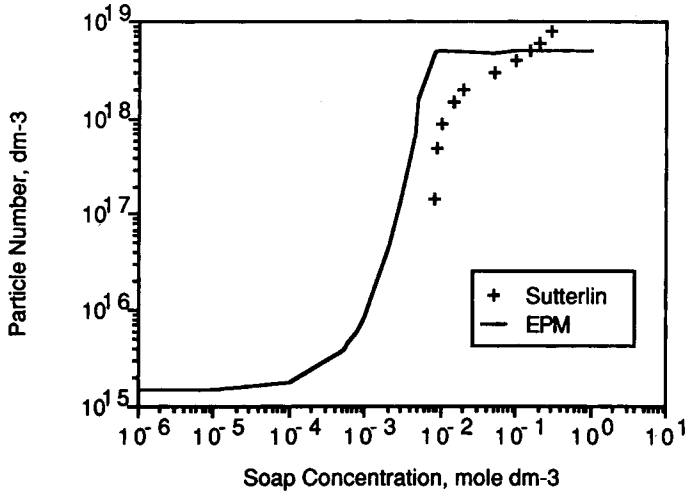

Fig. 5. Particle number vs. soap concentration for the data of Sütterlin[36] (+): (−) EPM.

Data of Goodwin et al.[35]

Figure 2 shows the dependence of the calculated and the measured particle number on the ionic strength of the emulsion. The initiator (potassium persulfate) concentration was held constant at 0.00276 mol dm^{-3}. The ionic strength was varied by manipulating the concentration of the added electrolyte (sodium chloride). As the ionic strength of the emulsion is increased the coagulative nucleation mechanism predicts the formation of fewer particles in accordance with the experimental observations.

Figure 3 shows the dependence of the calculated and the measured particle number on the initiator concentration. In these data, the ionic strength of the emulsion was maintained constant at 0.0113 mol dm^{-3} by adjusting the sodium chloride concentration for different initiator concentrations. There is

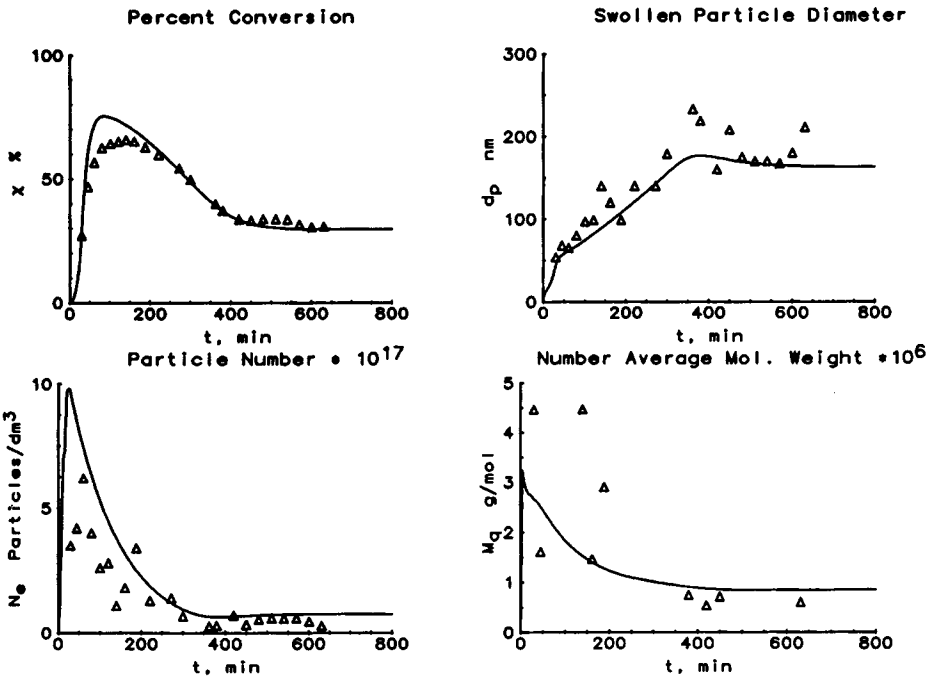

Fig. 6. Conversion, swollen particle diameter, particle number, and molecular weight vs. time for the data of Badder and Brooks.[37]

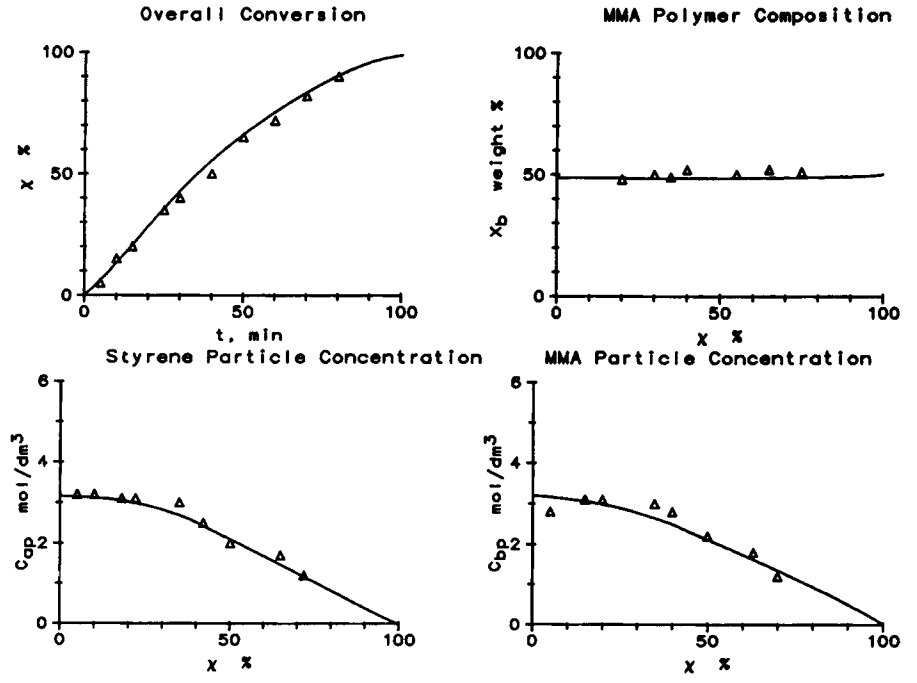

Fig. 7. Overall conversion vs. time, and polymer composition, styrene concentration in the particles, and MMA concentration in the particles vs. overall conversion for the data of Nomura and Fujita.[11] Initial weight ratio (MMA/total monomer) = 0.5.

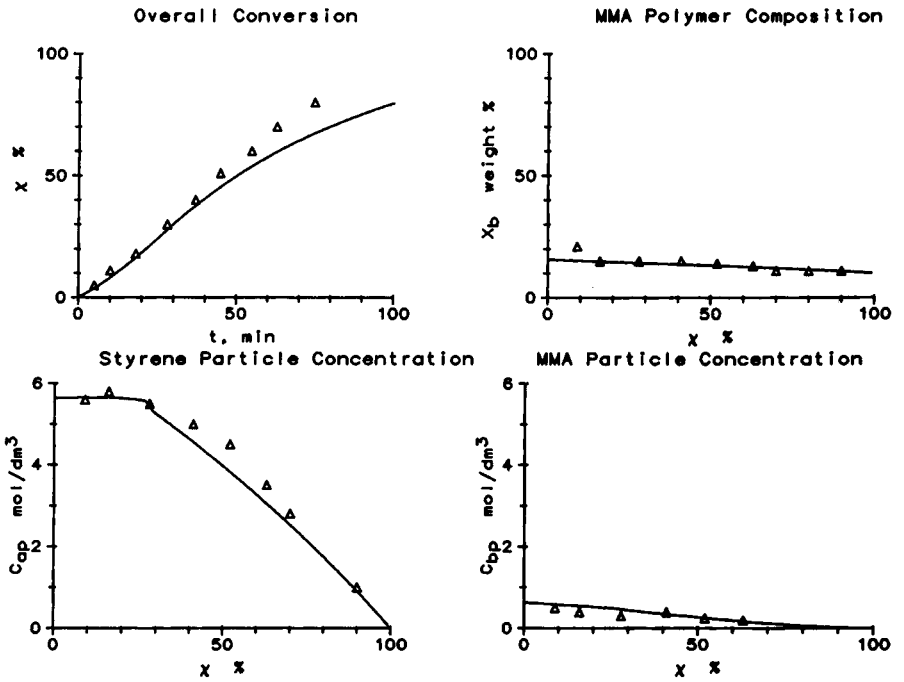

Fig. 8. Overall conversion vs. time, and polymer composition, styrene concentration in the particles, and MMA concentration in the particles vs. overall conversion for the data of Nomura and Fujita.[11] Initial weight ratio (MMA/total monomer) = 0.1.

generally good agreement between EPM and experiment, although there is a small overprediction of the particle concentration at low initiator concentrations. The same good agreement with the data of Goodwin et al.[35] has been obtained by Feeney et al.[8]

Data of Sütterlin[36]

Figure 4 shows that EPM is also able to predict the classical Smith–Ewart[5] dependence of the particle number on initiator concentration at high levels of added surfactant (sodium dodecylsulfate = 0.1 mol dm^{-3}).

Figure 5 shows that EPM is able to reproduce fairly well the experimentally observed dependence of the particle number on surfactant concentration at a fixed initiator concentration (ammonium persulfate = 0.00317 mol dm^{-3}). An important feature of EPM is that it calculates the coefficient for the entry rate of oligomeric free radicals into polymer particles and precursors by using surface diffusion and coagulative entry. The entry rate coefficient therefore decreases as the amount of surfactant is increased yielding higher homogeneous nucleation rates at the high surfactant concentrations. At very low surfactant concentrations, the particle number is independent of added surfactant (since the colloidal stability arises solely from surfactant generated *in situ*). As more surfactant is added, the particle number increases significantly, because the surfactant stabilizes the precursors and reduces the rate of coagulation. Our model predicts that the particle number finally levels off at very high concentrations of added surfactant, since the surface of the particles

TABLE I
Base Case Parameters for Simulations

Symbol	Value	Reference
	Parameters for styrene	
k_{paa}	$= 1.259 \times 10^7 \exp(-29 \text{ kJ mol}^{-1}/RT_e) \text{ dm}^3 \text{ mol}^{-1} \text{ s}^{-1}$	40
k_{taa0}	$= 1.7 \times 10^9 \exp(-9 \text{ kJ mol}^{-1}/RT_e) \text{ dm}^3 \text{ mol}^{-1} \text{ s}^{-1}$	40
k_{taa1}	$= -2.57 + 5.05 \times 10^{-3} T_e$	21
k_{taa2}	$= -9.56 + 1.76 \times 10^{-2} T_e$	21
k_{taa3}	$= 3.03 - 7.85 \times 10^{-3} T_e$	21
k_{xaa}	$= 2.512 \times 10^6 \exp(-53 \text{ kJ mol}^{-1}/RT_e) \text{ dm}^3 \text{ mol}^{-1} \text{ s}^{-1}$	4
k_{ma}	$= 10. \times 10^{-8} \text{ m s}^{-1}$	26
D_{wa}	$= 1.2 \times 10^{-9} \text{ m}^2 \text{ s}^{-1}$	11
D_{pa}	$= 1. \times 10^{-11} \text{ m}^2 \text{ s}^{-1}$	41
α_a	$= 0.0$	42
ρ_{T_e}	$= 1. \times 10^{13} \exp(-105 \text{ kJ mol}^{-1}/RT_e) \text{ s}^{-1}$	4
ρ_a	$= 0.903 \text{ g dm}^{-3}$	43
C_{aw}^{sat}	$= 3.68 \times 10^{-3} \text{ mol dm}^{-3}$ ($T_e = 50°\text{C}$)	44
	$= 4.0 \times 10^{-3} \text{ mol dm}^{-3}$ ($T_e = 70, 80°\text{C}$)	44
K_{awp}	$= 5.88 \times 10^{-4}$	10
	Parameters for methyl methacrylate ($T_e = 50°\text{C}$)	
k_{pbb}	$= 580 \text{ dm}^3 \text{ mol}^{-1} \text{ s}^{-1}$	45
k_{tbb0}	$= 3.29 \times 10^7 \text{ dm}^3 \text{ mol}^{-1} \text{ s}^{-1}$	40
k_{tbb1}	$= -41.54 + 0.1082 T_e$	21
k_{tbb2}	$= 23.46 - 0.0785 T_e$	21
k_{tbb3}	$= 0.0$	21
k_{xbb}	$= 2.32 \times 10^{-2} \text{ dm}^3 \text{ mol}^{-1} \text{ s}^{-1}$	45
k_{mb}	$= 2.7 \times 10^{-8} \text{ m s}^{-1}$	4
D_{wb}	$= 1.7 \times 10^{-9} \text{ m}^2 \text{ s}^{-1}$	11
D_{pb}	$= 1. \times 10^{-11} \text{ m}^2 \text{ s}^{-1}$	41
α_b	$= 1.0$	45
ρ_b	$= 0.93 \text{ g dm}^{-3}$	43
C_{bw}^{sat}	$= 0.156 \text{ mol dm}^{-3}$	1
K_{bwp}	$= 2.2 \times 10^{-2}$	10
	Parameters for styrene / methyl methacrylate	
r_a	$= k_{paa}/k_{pab} = 0.501$	46
r_b	$= k_{pbb}/k_{pba} = 0.472$	46
ρ_q	$= 1.111 \text{ g dm}^{-3}$	41
	Parameters for ammonium and potassium persulfate	
k_i	$= 2.288 \times 10^{16} \exp(-137.9 \text{ kJ mol}^{-1}/RT_e) \text{ s}^{-1}$	47
ρ_i	$= 1.98 \text{ g dm}^{-3}$	43
	Parameters for sodium dodecyl sulfate	
a_s'	$= 43 \text{ Å}^2 \text{ molecule}^{-1}$	38
b_s	$= 2400 \text{ dm}^3 \text{ mol}^{-1}$	38
ρ_s	$= 1.4 \text{ g dm}^{-3}$	43
	Parameters for water	
ϵ_r	$= 70$	43
μ	$= 3 \times 10^{-4} \text{ kg m}^{-1} \text{ s}^{-1}$	43
	Parameters for coagulative nucleation	
A	$= 6.5 \times 10^{-21} \text{ J}$	28
a_g'	$= 43 \text{ Å}^2 \text{ molecule}^{-1}$	This work
b_g	$= 50 \text{ dm}^3 \text{ mol}^{-1}$	This work
δ	$= 1.41 \text{ Å}$	8
m	$= 21$	8
$\bar{n}_v$	$= 0.1$	8
r_{FH}	$= 15 \text{ nm}$	8
r_1	$= 1 \text{ nm}$	This work
β_e	$= 1$	This work
ω	$= 1$	29
k_{ea}^{max}	$= 2 \times 10^8 \text{ dm}^3 \text{ mol}^{-1} \text{ s}^{-1}$	This work

will always be completely covered with surfactant if the surfactant concentration is above a certain minimal value dictated by the adsorption isotherm parameters. Sütterlin's data for methyl acrylate clearly show this predicted S-shape curve. However, his styrene data (Fig. 5) do not show evidence for the predicted S-shaped curve. In the absence of data at higher surfactant concentration (which is unobtainable for sodium dodecylsulfate because of its limited solubility at the temperature studied), all that can be said is that the styrene data are not inconsistent with our predictions. It should also be noted that Sütterlin's results for methyl acrylate refute the prediction of the micellar entry model, which says that no leveling off should ever be observed. Since the data for methyl acrylate do show the predicted leveling-off effect, we suspect that the trend is a general one.

In generating the S-shaped curve for Sütterlin[36] (Fig. 5), the Langmuir isotherm "clinging" parameter b_s was changed from 2400 $dm^3\ mol^{-1}$ as measured by Ahmed et al.[38] at 25°C to 50 $dm^3\ mol^{-1}$ so that the steep part of the curve would occur closer to the data. This difference may perhaps be ascribed to the greatly differing temperatures (the Sütterlin data are at 80°C), since the factors that govern b_S will certainly have a strong enthalpic component. Another possible origin for this difference may be the dependence of the adsorption isotherm parameters on particle size: We are here mainly concerned with very small precursor particles, whereas the data of Ahmed et al.[38] are for particles whose radius is an order of magnitude greater.

Prindle and Ray[39] have recently analyzed the same styrene data using a hybrid model consisting of the micellar nucleation mechanism above the critical micelle concentration (CMC) and of the homogeneous nucleation and coagulation mechanism below the CMC. Their simulations show a much steeper rise in the particle number concentration right at the CMC than predicted by EPM. Their hybrid model does not appear to predict that the particle concentration levels off at high surfactant concentrations.

Data of Badder and Brooks[37]

Figure 6 shows the comparisons of EPM with the experimental data obtained by Badder and Brooks[37] in a CSTR (run C-24). The reactor feed contained 22.8% styrene, 0.64% emulsifier (sodium dodecylsulfate), and 0.39% initiator (ammonium persulfate). The residence time was 114 min. The initial reactor charge was water and emulsifier. In this case the size of the primary precursors was varied slightly from its baseline value (0.8 nm). Although the experimental data show some scatter, EPM reproduces very well both the transient and steady state behavior of the particle number, the average swollen particle diameter, the overall conversion, and the number average molecular weight.

Data of Nomura and Fujita[11]

The predictive capabilities of EPM for copolymerizations are shown in Figures 7 and 8. Nomura has published a very extensive set of seeded experimental data for the system styrene-MMA. Figures 7 and 8 summarize the EPM calculations for two of these runs which were carried out in a batch reactor at 50°C at an initiator concentration of 1.25 g dm^{-3} water. The

concentration of the seeded particles was $6 \times 10^{17}\,dm^{-3}$ and the total mass of monomer was 200 g dm^{-3}. The ratio of the mass of MMA to the total monomer was 0.5 and 0.1 in Figures 7 and 8, respectively. The value of β_e in eqs. (66) and (67) was changed from one to zero for these runs, because the mass transfer term ($4\pi r_p^2 k_{ma} N_A$) by itself predicted satisfactorily the entry rate coefficients k_{ea} and k_{eb} and the initiator efficiency f. The agreement between the measured and predicted values of the total monomer conversion, the copolymer composition, and the concentration of the two monomers in the latex particles is excellent. The transition from interval II to interval III is predicted satisfactorily. In accordance with the experimental observations, EPM predicted no new particle formation under the conditions of this run.

CONCLUSIONS

Emulsion polymerization is a complicated physicochemical process that has challenged researchers for many years. The emulsion polymerization model presented here is able to reproduce an extremely wide range of data with a single, internally consistent model. It (i) successfully predicts the variation over 4 orders of magnitude of the particle number as the surfactant concentration ranges from zero to a high value (well above the CMC), and in particular the S-shaped curve observed experimentally for this dependence, which is quite contradictory to the predictions of older theories such as micellar entry; it (ii) predicts the dependence of particle number on ionic strength and initiator concentration; it (iii) gives quite acceptable accord with batch and CSTR reactor conversion, particle size, and molecular weight data; (iv) copolymerization data are also successfully modeled; and (v) other work[7,8] has shown that the same homopolymerization model successfully predicts particle size distributions.

The extensive verification of the model structure on the well-characterized styrene and styrene/MMA polymerizations has allowed us to use the same structure to obtain fundamental insights into emulsion polymerizations involving other monomers of significant importance to DuPont.

The authors would like to thank W. D. Smith, Jr. for his support of this work. One of us R. G. G. gratefully acknowledges many stimulating and insightful discussions with Professor Don Napper. The authors would also like to thank Jean M. Richards for her patience and support.

APPENDIX: NOMENCLATURE

Latin Upper Case Variables

A	area, Hamaker constant, Arrhenius preexponential factor
A	monomer A
B	Müller coagulation coefficient
B	monomer B
C	concentration
D	diffusivity
E	activation energy
F	molar flow rate
G	particle formation rate
H	enthalpy
I	ionic strength, modified Bessel function

I	initiator
K	partition coefficient, volumetric growth rate
L_{ij}	surface to surface distance
M	molecular weight
N	number concentration of particles
N_A	Avogadro's number
Q	volumetric flow rate
Q	dead polymer
R	Reaction rate, gas constant
R_{ij}	center to center distance
T	temperature
U	heat transfer coefficient
V	volume
W	stability ratio
X	weight fraction
X	chain transfer agent
Y	added electrolyte

Latin Lower Case Variables

a	area per molecule in Langmuir isotherm
b	Langmuir isotherm constant
c	termination coefficient, heat capacity
e	base of natural logarithms
e_L	electron charge
f	initiator efficiency
j	chain length
k	kinetic rate constant
k_B	Boltzmann constant
m	number of precursors in a latex particle
n	number of radicals per particle
$\bar{n}$	average number of radicals per particle
r	radius
r_{FH}	Flory–Huggins radius
t	time
v	number concentration of precursors
z	ionic valence

Greek Variables

α	fate parameter
β	coagulative entry switch
γ	ratio of $C_{a\cdot}$ to $C_{b\cdot}$ radical concentrations
δ	Stern layer thickness
Δ	Difference operator
ϵ_0	permittivity of the vacuum
ϵ_r	dielectric constant
ζ	zeta potential
θ	fractional surface coverage
κ	inverse electric double layer thickness
λ	intermediate variable
μ	viscosity
ν	order of the modified Bessel function in the O'Toole equation
ξ	argument of the modified Bessel function in the O'Toole equation
ρ	density, radical entry rate per particle
σ	surface charge density
τ	filter factor
υ	volume of a particle or precursor

ϕ volume fraction
Φ potential energy
χ conversion
ψ surface electric potential
ω fraction of charged end groups on particle surface

Subscripts and Superscripts

a monomer A
b monomer B
cr critical
d desorption
e entry, emulsion
f feed
g generated surfactant
h homogeneous
i indices
i initiator
I ionic end groups
j indices, jacket
k indices
m monomer, mass transfer
max maximum
n number of radicals per particle
o overall, standard value
p swollen polymer phase, propagation
q dead polymer
r radicals
s added surfactant
sat saturated
t termination
T total, thermal
v precursor particles
w aqueous phase
x chain transfer
y added electrolyte
z_+ Valence
radical species
0 initial condition

References

1. J. B. Rawlings and W. H. Ray, *Polym. Eng. Sci.*, **28**(5), 237 (1988).
2. K. W. Min and W. H. Ray, *J. Macromol. Sci., Rev Macromol. Chem.*, **C1**, 177 (1974).
3. A. Penlidis, J. F. MacGregor, and A. E. Hamielec, *AIChE J.*, **31**, 881 (1985).
4. R. G. Gilbert and D. H. Napper, *J. Macromol. Sci., Rev. Macromol. Chem. Phys.*, **C23**, 127 (1983).
5. W. V. Smith and R. H. Ewart, *J. Chem. Phys.*, **16**, 592 (1948).
6. F. K. Hansen and J. Ugelstad, *J. Polym. Sci., Polym. Chem. Ed.*, **16**, 1953 (1978).
7. P. J. Feeney, D. N. Napper, and R. G. Gilbert, *Macromolecules*, **17**, 2520 (1984).
8. P. J. Feeney, D. H. Napper, and R. G. Gilbert, *Macromolecules*, **20**, 2922 (1987).
9. V. C. Haskell and P. H. Settlage, in *Polymer Colloids I*, R. M. Fitch, Ed., Plenum, New York, 1971, p. 583.
10. T. O. Broadhead, A. E. Hamielec, and J. F. MacGregor, *Makromol., Chem., Suppl.* **10 / 11**, 105 (1985).
11. M. Nomura and K. Fujita, *Makromol. Chem. Suppl.*, **10 / 11**, 25 (1985).
12. E. P. Dougherty, *J. Appl. Polym. Sci.*, **32** 3051 (1986).
13. E. P. Dougherty, *J. Appl. Polym. Sci.* **32** 3079 (1986).

14. G. Storti, L. Vitalini, M. Albano, S. Carrà, and M. Morbidelli, *IUPAC Symp. S. Margherita Ligure (Italy)*, **17**, 214 (1987).

15. J. P. Congalidis, J. R. Richards, and R. G. Gilbert, in *International Symposium on Computer Applications in Applied Polymer Science*, 195th ACS Meeting, Toronto, 1988, ACS Symposium Series, to appear.

16. F. K. Hansen and J. Ugelstad, in *Emulsion Polymerization*, I. Piirma, Ed., Academic, New York, 1982, p. 51.

17. P. J. Feeney, R. G. Gilbert, and D. H. Napper, *J. Colloid Interfacial Sci.*, **107**, 159 (1985).

18. P. J. Feeney, E. Geissler, R. G. Gilbert, and D. H. Napper, *J. Colloid Interfacial Sci.*, **118**, 493 (1987).

19. P. J. Flory, *Principles of Polymer Chemistry*, Cornell University Press, Ithaca, NY, 1953

20. W. R. Krigbaum and D. K. Carpenter, *J. Polym. Sci.*, **14** 241 (1954).

21. N. Friis and A. E. Hamielec, *Am. Chem. Soc. Symp. Ser.*, **24**, 82 (1976).

22. G. T. Russell, D. H. Napper, and R. G. Gilbert, *Macromolecules*, **21**, 2133 (1988).

23. F. K. Hansen and J. Ugelstad, *Makromol. Chem.*, **180**, 2423 (1979).

24. J. T. O'Toole, *J. Appl. Polym. Sci.*, **9**, 1291, (1965).

25. J. Ugelstad, P. C. Moek, and J. O. Aasen, *J. Polym. Sci., A-1*, **5**, 2281 (1967).

26. I. A. Penboss, R. G. Gilbert, and D. H. Napper, *J. Chem. Soc. Faraday Trans. I*, **82**, 2247 (1986).

27. J. Th. G. Overbeek, in *Colloid Science*, H. R. Kruyt, Ed., Elsevier, Amsterdam, 1952.

28. R. H. Ottewill, in *Emulsion Polymerization*, I. Piirma, Ed., Academic, New York, 1982, p. 1.

29. H. J. van den Hul and J. W. Vanderhoff, in *Polymer Colloids I*, R. M. Fitch, Ed., Plenum, New York, 1971, p. 1.

30. A. S. Dunn and L. C.-H. Chong, *Br. Polym. J.*, **2**, 49 (1970).

31. H. C. Hamaker, *Physica*, **4**, 1058 (1937).

32. R. Hogg, T. W. Healy, and D. W. Fuerstenau, *Trans. Faraday Soc.*, **62**, 1638 (1966).

33. H. Müller, *Kolloid.-Beih.* **26**, 257 (1928).

34. *Numerical Algorithms Group Library Manual*, Routines C05NBF, D02EBF, E04ABF, Vol. 1, 1984.

35. J. W. Goodwin, J. Hearn, C. C. Ho, and R. H. Ottewill, *Colloid Polym. Sci.*, **252**, 464 (1974).

36. N. Sütterlin, in *Polymer Colloids II*, R. M. Fitch, Ed., Plenum, New York, 1980, p. 583.

37. E. E. Badder and B. W. Brooks, *Chem. Eng. Sci.*, **39**, 1499 (1984).

38. S. M. Ahmed et al., in *Polymer Colloids II*, R. M. Fitch, Ed., Plenum, New York, 1980, p. 265.

39. J. C. Prindle and W. H. Ray, presented at the AIChE Annual Meeting, New York, 1987.

40. M. Buback, L. H. Garcia-Rubio, R. G. Gilbert, and D. H. Napper, J. Guillot, A. E. Hamielec, D. Hill, K. F. O'Driscoll, O. F. Olaj, Jiacong Shen, D. Solomon, G. Moad, M. Stickler, M. Tirrell, and M. A. Winnik, *J. Polym. Sci., Polym. Lett. Ed.*, **26**, 293 (1988).

41. J. Brandrup and E. H. Immergut, *Polymer Handbook*, Wiley-Interscience, New York, 1975.

42. B. S. Hawkett, D. H. Napper, and R. G. Gilbert, *J. Chem. Soc. Faraday Trans. I*, **76**, 1323 (1980).

43. R. H. Perry, *Chemical Engineers' Handbook*, 6th ed., McGraw-Hill, New York, 1984.

44. F. A. Bovey and I. M. Kolthoff, *J. Polym. Sci.*, **5**, 487 (1950).

45. M. J. Ballard, D. H. Napper, and R. G. Gilbert, *J. Polym. Sci., Polym. Chem. Ed.*, **22**, 3225 (1984).

46. R. Leicht and J. Fuhrman, *J. Polym. Sci.*, **21**, 2215 (1983).

47. I. M. Kolthoff and I. K. Miller, *J. Am. Chem. Soc.*, **73**, 3055 (1951).

Received February 16, 1988
Accepted June 1, 1988